Available online at www.elixirpublishers.com (Elixir International Journal)

Applied Mathematics

Elixir Appl. Math. 97 (2016) 42304-42311

ISSN: 2229-712X

Numerical Study on Unsteady MHD Free Convection and Mass Transfer Flow Past a Vertical Flat Plate in Porous Medium, Chemical Reaction and Soret Effects

M. K. Das, P. Biswas, A. Rahman and S. F. Ahmmed

Mathematics Discipline, Khulna University, Khulna-9208, Bangladesh.

ARTICLE INFO

Article history:

Received: 14 June 2016;

Received in revised form: 16 August 2016;

Accepted: 26 August 2016;

Keywords

MHD,
Mass transfer,
Natural Convection,
Flat Plate,
Chemical Reaction,
Porous Medium.

ABSTRACT

A two dimensional unsteady MHD free convection and mass transfer flow of an incompressible, viscous and electrically conducting fluid past an accelerated vertical flat plate through porous medium with chemical reaction, heat source, thermal diffusion and the influence of uniform magnetic field applied normal to the plate has been studied. The solution would be based mainly on finite difference methods. The system of equations has been transformed into a dimensionless form by using well known transformations. The dimensionless continuity, momentum, energy and concentration equations are solved numerically by explicit finite difference technique. The results for velocity, temperature, concentration, streamlines, isotherm lines are discussed graphically and the skin friction, Nusselt number are described in tables with different time steps as well as for different values of flow parameters of physical and engineering interest.

Introduction

MHD flow problems have become in view of its significant applications in industrial manufacturing processes such as plasma studies, petroleum industries, magneto hydrodynamics power generator cooling of clear reactors, cooling towers, MHD pumps, MHD bearings, boundary layer control in aerodynamics etc. Many authors have studied the effects of chemical reaction, Soret number, magnetic field on mixed, natural and force convection heat and mass transfer problems.

Free convection flow is often encountered in cooling of nuclear reactors or in the study of structure of stars and planets. Along with the free convection flow the phenomenon of mass transfer is also very common in the theories of stellar structure. Convection in porous media has applied in geothermal energy recovery, oil extraction, thermal energy storage and flow through filtering devices. Many research works have been done in the field of chemical reaction, heat and mass transfer. The study of heat and mass transfer with chemical reaction is of great practical importance to engineers and scientists because of its almost universal occurrence in many branches of science and engineering.

Several researchers have studied the problem of MHD free convection flow with mass transfer. The implicit finite difference method is used to obtain the solution of radiation effects on MHD unsteady free convection flow on vertical porous plate by Abd EL-Naby et al. [1]. S. F. Ahmmed and M. K. Das [2] have studied unsteady MHD free convection and mass transfer flow past a vertical porous plate. Mass transfer effects on MHD flow and heat transfer past a vertical porous plate through porous medium under oscillatory suction and heat source have been investigated by S. S. Das et al. [3]. The soret effects on free convective unsteady MHD flow over a vertical plate with heat source have been studied by M. Bhavana et al. [4]. M. M. Alam et al. [5] have studied the micro-polar fluid behavior on MHD heat transfer flow through a porous medium with induced magnetic field by finite difference method. H. S. Takhar et al. [6] also have discussed the transient free convection past a semi-infinite vertical plate with variable surface temperature. Effects of chemical reactions on free convection MHD flow past an exponentially accelerated infinite vertical plate through a porous medium with variable temperature and mass diffusion have been analyzed by U. S. Rajput et al. [7]. J. Girish Kumar et al. [8] have paid attention to the mass transfer effects on MHD flows exponentially accelerated isothermal vertical plate in the presence of chemical reaction through porous medium. M. S. Hossain et al. [9] have discussed the MHD free convection heat and mass transfer flow past a vertical plate in the presence of hall current. N. Vedavathi et al. [10] have studied the radiation and mass transfer effects on unsteady MHD convective flow past an infinite vertical plate as well as Dufour and Soret effects on it. Similar work as the nature of vertical natural convection flows resulting from the combined buoyancy effects of thermal and mass diffusion have been performed in 1971 by B. Gebhart et al. [11]. And S. F. Ahmmed et al. [12] have been studied MHD free convection and mass transfer flow past a vertical flat plate in the presence of heat source, thermal diffusion, large suction and the influence of uniform magnetic field.

Here we have investigated the unsteady MHD free convection boundary layer flow of a viscous incompressible fluid past a vertical flat plate with effect of heat source

Tele:
E-mail address: sfahmmed@yahoo.com

parameter, chemical reaction and Soret number. Then the problem is formulated and solved numerically.

The obtained results for the velocity, temperature, concentration fields, the streamlines and isotherm lines are represented graphically.

Formulation of the problem

Consider a two dimensional unsteady flow of an incompressible, electrically conducting and viscous fluid past a continuously moving vertical flat plate through porous medium and subjected to a uniform transverse magnetic field. According to the coordinate system the x'- axis is chosen along the plate in the direction of flow and y'- axis normal to it. The plate is maintained at a constant temperature T'_w and the concentration is maintained at a constant value C'_w. The temperature of ambient flow is T'_∞ and the concentration of uniform flow is C'_∞. It is assumed that there is no applied voltage of which implies the absence of an electric field. Transversely applied magnetic field and magnetic Reynolds number are very small. For which the induced magnetic field is negligible. Considering the joule heating and viscous dissipation terms to negligible the magnetic field is not enough to cause joule heating, so the term due to electrical dissipation is neglected in the energy equation. By usual Boussinesq's approximation, the unsteady flow is governed by the following equations:

$$\frac{\partial u'}{\partial x'}+\frac{\partial v'}{\partial y'}=0 \tag{1}$$

$$\frac{\partial u'}{\partial t'}+u'\frac{\partial u'}{\partial x'}+v'\frac{\partial v'}{\partial y'}=\upsilon\frac{\partial^2 u'}{\partial y'^2}+g\beta\left(T'-T'_\infty\right)+g\beta_c\left(C'-C'_\infty\right)-\frac{\sigma B_0^2 u'}{\rho}-\frac{u'}{k'} \tag{2}$$

$$\frac{\partial u'}{\partial t'}+u'\frac{\partial T'}{\partial x'}+v'\frac{\partial T'}{\partial y'}=\frac{k}{\rho C_p}\frac{\partial^2 T'}{\partial y'^2}+\frac{Q_0}{\rho C_p}\left(T'-T'_\infty\right) \tag{3}$$

$$\frac{\partial C'}{\partial t'}+u'\frac{\partial C'}{\partial x'}+v'\frac{\partial C'}{\partial y'}=D_M\frac{\partial^2 C'}{\partial y'^2}+D_T\frac{\partial^2 C'}{\partial y'^2}-R'\left(C'-C'_\infty\right) \tag{4}$$

With boundary conditions,

$$\begin{aligned} &u'=U_0,\ v'=0,\ T'=T'_w,\ C'=C'_w && \text{at } y'=0\\ &u'=0,\ v'=0,\ T'=T'_\infty,\ C'=C'_\infty && \text{as } y'\to\infty \end{aligned} \tag{5}$$

Where u' and v' are velocity components along x'- axis and y'-axis respectively, g is acceleration due to gravity, T' is the temperature, k is thermal conductivity, σ is the electrical conductivity, D_M is the molecular diffusivity, U_0 is the uniform velocity, C' is the concentration of the species, B_0 is the uniform magnetic field, C_p is the specific heat at constant pressure, Q_0 is the constant heat source, D_T is the thermal diffusivity, ρ is the density, υ is the kinematic viscosity, β is the volumetric coefficient of thermal expansion and β_c is the volumetric coefficient of thermal expansion with concentration and other symbols have their usual meaning.

To get the solution of the equation (1) to equation (4) with boundary condition (5), we introduce the following non-dimensional quantities and parameters

$$\begin{aligned} &t=\frac{t'U_0^2}{\upsilon},\ X=\frac{x'U_0}{\upsilon},\ Y=\frac{y'U_0}{\upsilon},\ U=\frac{u'}{U_0},\ V=\frac{v'}{U_0},\\ &T'=T'_\infty+\left(T'_w-T'_\infty\right)T,\ C'=C'_\infty+\left(C'_w-C'_\infty\right)C,\\ &Gr=\frac{g\beta\upsilon\left(T'_w-T'_\infty\right)}{U_0^3},\ Gm=\frac{g\beta_c\upsilon\left(C'_w-C'_\infty\right)}{U_0^3},\\ &M=\frac{\sigma B_0^2\upsilon}{\rho U_0^2},\ K=\frac{U_0^2 k'}{\upsilon^2},\ R=\frac{R'\upsilon}{U_0^2},\ Sc=\frac{\upsilon}{D_M} \end{aligned} \tag{6}$$

Therefore, the governing equations in the dimensionless form become equation (7) to equation (10) with the boundary condition (11),

$$\frac{\partial U}{\partial X}+\frac{\partial V}{\partial Y}=0 \tag{7}$$

$$\frac{\partial U}{\partial t}+U\frac{\partial U}{\partial X}+V\frac{\partial U}{\partial Y}=\frac{\partial^2 U}{\partial Y^2}+GrT+GmC-\left(M+\frac{1}{K}\right)U \tag{8}$$

$$\frac{\partial T}{\partial t}+U\frac{\partial T}{\partial X}+V\frac{\partial T}{\partial Y}=\frac{1}{Pr}\frac{\partial^2 T}{\partial Y^2}+ST \tag{9}$$

$$\frac{\partial C}{\partial t}+U\frac{\partial C}{\partial X}+V\frac{\partial C}{\partial Y}=\frac{1}{Sc}\frac{\partial^2 C}{\partial Y^2}+S_0\frac{\partial^2 T}{\partial Y^2}-RC \tag{10}$$

The corresponding initial and boundary conditions are

$$\begin{aligned} &U=1,\ V=0,\ T=1,\ C=1 && \text{at } Y=0\\ &U=0,\ V=0,\ T=0,\ C=0 && \text{as } Y\to\infty \end{aligned} \tag{11}$$

It is now important to calculate the physical quantities of primary interest, which are the local wall shear stress, the local surface heat flux. Given the velocity field in the boundary layer, we can calculate the local wall shear stress i.e., skin friction as

$$\mu\left(\frac{\partial u'}{\partial y'}\right)_{y'=0}$$

and in dimensionless form, we obtain

$$C_f=\left(\frac{\partial U}{\partial Y}\right)_{Y=0}$$

The local Nusselt number is defined as

$$-\left(\frac{\partial T'}{\partial y'}\right)_{y'=0}$$

So the dimensionless Nusselt number is

$$-\left(\frac{\partial T}{\partial Y}\right)_{Y=0}$$

We can calculate the stream function from the following equations as satisfying continuity equation (7).

$$U=\frac{\partial\psi}{\partial Y}\quad\text{and}\quad V=-\frac{\partial\psi}{\partial X}$$

We can obtain the streamlines from the following expressions as described in the beneath

$$\psi=\int_0^{Y_{\max}} U\,dY$$

Numerical solutions

Systems of non-linear coupled partial differential equations with the boundary conditions are very difficult to solve analytically. For simplicity the explicit finite difference method has been used to solve equation (7) to equation (10) subject to the boundary conditions (11). In this case the region within the boundary layer is divided by some perpendicular lines of *Y*- axis, where *Y*- axis is normal to the medium.

It should be noted that the maximum length of boundary layer is $Y_{\max}$ (=25) as corresponds to $Y\to\infty$

i.e. *Y* varies from 0 to 25. And the number of grid spacing in *Y* directions is *m* (=100), hence the constant mesh size along *Y* axis becomes $\Delta Y= 0.25$ $(0 \le Y \le 25)$ with the smaller time step $\Delta t = 0.001$.

Using the finite difference method *U*, *T* and *C* can be represented in terms of the values of $U_{i,j}$, $T_{i,j}$ and $C_{i,j}$ at the end of the time step respectively. Explicit finite difference approximation gives,

$$\left(\frac{\partial U}{\partial t}\right)_{i,j} = \frac{U'_{i,j} - U_{i,j}}{\Delta t},\ \left(\frac{\partial U}{\partial X}\right)_{i,j} = \frac{U_{i,j} - U_{i-1,j}}{\Delta X},$$

$$\left(\frac{\partial U}{\partial Y}\right)_{i,j} = \frac{U_{i,j+1} - U_{i,j}}{\Delta Y},\ \left(\frac{\partial V}{\partial Y}\right)_{i,j} = \frac{V_{i,j} - V_{i,j-1}}{\Delta Y},$$

$$\left(\frac{\partial T}{\partial t}\right)_{i,j} = \frac{T'_{i,j} - T_{i,j}}{\Delta t},\ \left(\frac{\partial T}{\partial X}\right)_{i,j} = \frac{T_{i,j} - T_{i-1,j}}{\Delta X},$$

$$\left(\frac{\partial T}{\partial Y}\right)_{i,j} = \frac{T_{i,j+1} - T_{i,j}}{\Delta Y},\ \left(\frac{\partial C}{\partial t}\right)_{i,j} = \frac{C'_{i,j} - C_{i,j}}{\Delta t},$$

$$\left(\frac{\partial C}{\partial X}\right)_{i,j} = \frac{C_{i,j} - C_{i-1,j}}{\Delta X},\ \left(\frac{\partial C}{\partial Y}\right)_{i,j} = \frac{C_{i,j+1} - C_{i,j}}{\Delta Y},$$

$$\left(\frac{\partial^2 U}{\partial Y^2}\right)_{i,j} = \frac{U_{i,j+1} - 2U_{i,j} + U_{i,j-1}}{(\Delta Y)^2},\quad \psi_{i,j} = \psi_{i,j+1} - U_{i,j}\Delta Y$$

$$\left(\frac{\partial^2 T}{\partial Y^2}\right)_{i,j} = \frac{T_{i,j+1} - 2T_{i,j} + T_{i,j-1}}{(\Delta Y)^2},$$

$$\left(\frac{\partial^2 C}{\partial Y^2}\right)_{i,j} = \frac{C_{i,j+1} - 2C_{i,j} + C_{i,j-1}}{(\Delta Y)^2}$$

Substituting the above relations into the corresponding partial differential equation (7) to equation (10), an appropriate set of finite difference equation have been made as

Continuity equation

$$\frac{U_{i,j} - U_{i-1,j}}{\Delta X} + \frac{V_{i,j} - V_{i,j-1}}{\Delta Y} = 0 \tag{12}$$

Momentum equation

$$\frac{(U'_{i,j} - U_{i,j})}{\Delta t} + U_{i,j}\frac{U_{i,j} - U_{i-1,j}}{\Delta X} + V_{i,j}\frac{V_{i,j} - V_{i,j-1}}{\Delta Y} = \frac{U_{i,j+1} - 2U_{i,j} + U_{i,j-1}}{(\Delta Y)^2} + Gr\,\theta_{i,j} + Gm\,\phi_{i,j} - \left(M + \frac{1}{K}\right)U_{i,j} \tag{13}$$

Energy equation

$$\frac{T'_{i,j} - T_{i,j}}{\Delta t} + U_{i,j}\frac{T_{i,j} - T_{i-1,j}}{\Delta X} + V_{i,j}\frac{T_{i,j+1} - T_{i,j}}{\Delta Y} = \frac{1}{Pr}\frac{T_{i,j+1} - 2T_{i,j} + T_{i,j-1}}{(\Delta Y)^2} + ST_{i,j} \tag{14}$$

Concentration equation

$$\frac{C'_{i,j} - C_{i,j}}{\Delta t} + U_{i,j}\frac{C_{i,j} - C_{i-1,j}}{\Delta X} + V_{i,j}\frac{C_{i,j+1} - C_{i,j}}{\Delta Y} = \frac{1}{Sc}\frac{C_{i,j+1} - 2C_{i,j} + C_{i,j-1}}{(\Delta Y)^2} + S_0\frac{T_{i,j+1} - 2T_{i,j} + T_{i,j-1}}{(\Delta Y)^2} - RC_{i,j} \tag{15}$$

and the boundary condition with finite difference scheme as,

$$U^0_{i,j} = 1,\ V^0_{i,j} = 0,\ T^0_{i,j} = 1,\ C^0_{i,j} = 1 \quad \text{at} \quad Y = 0 \tag{16}$$

$$U^n_{i,j} = 0,\ V^n_{i,j} = 0,\ T^n_{i,j} = 0,\ C^n_{i,j} = 0 \ \text{as} \ Y \to \infty$$

Here the subscript *i* and *j* designate the grid points along *X* and *Y* coordinates respectively.

Results and discussion

We have obtained numerical results by solving the non-dimensional partial differential equations using explicit finite difference method. The effect of the flow parameters on the velocity, temperature, concentration, streamlines, isotherm lines distribution of the flow field are presented with the help of graphs. The initial value of the flow parameters are chosen as Gr=10, Gm=15, Sc=0.22, Pr=0.71, M=2, K=2, R=2, S_0=0.5 and S=0.5. To be realistic, the value of Schmidt number (Sc) are chosen for H_2 (Sc=0.22), CO_2 (Sc=0.30) and NH_3 (Sc=0.78). The value of Prandtl number (Pr) are chosen for air Pr=0.71, for stream Pr=1.0, for water Pr=7.02. The velocity profiles (U) for different values of the above parameters are illustrated in Figure 1 to Figure 8, the temperature profiles for different values of the flow parameters are displayed in Figure 9 to Figure 13 and the concentration profiles for different values of the above parameters are shown in Figure 14 to Figure 16. The streamlines and isotherm lines are described in Figure 17 to Figure 22 and Figure 23 to Figure 28 respectively. From the beneath described graphs it is clear that for the increasing time-steps velocities and temperatures are increased and mass concentration is decreased with different flow parameters.

Grashof number (Gr) approximates the ration of the buoyancy to viscous force acting on the fluid. When $Gr >>1$, the viscous force is negligible compared to the buoyancy and inertial forces. When buoyant forces overcome the viscous forces, the flow starts a transition to the turbulent regime. For a flat plate in vertical orientation, this transition occurs around $Gr=10e^9$. The velocity profile and temperature profile for different values of Grashof number (Gr) with different time-steps are described in Figure 1 and Figure 9. For the increasing value of Gr with increasing time increases the velocity and decreases temperature. Here the Grashof number leads free convection currents.

Figure 2 shows the effect of the modified Grashof number (Gm) on the velocity profile curves with various times. It is observed that an increasing in Gm leads to increase in the values of velocity. And it is noticed that for the time step t = 40 the effects of Gm on velocity is very small.

Figure 3 represents the velocity for different values of the permeability of porous medium (K). From the figure 3 it is noticed that the velocity tends to increase as permeability of porous medium (K) increases.

The effect of the magnetic field parameter (M) on the velocity profiles and temperature profiles are plotted in Figure 4 and Figure 10. This illustrates that the velocity decreases as the existence of magnetic field becomes stronger. This conclusion agrees with the fact that the magnetic field exerts retarding force on the free convection flow. From the Figure 10, for time-steps t = 1and t = 5 there is no effect of M on temperature but for the time-step t = 40 the temperature increases near the wall.

In heat transfer problems, the Prandtl number controls the relative thickness of the momentum and thermal boundary layers. When Pr is small, it means that the heat diffuses quickly compared to the velocity. This means that for liquid metals the thickness of the thermal boundary layer is much bigger than the velocity boundary layer. The velocity and temperature profiles for different values of Prandtl number (Pr) with different time-steps are exhibited in Figure 5 and Figure 11. It is observed that the effect of increasing values of Prandtl number (Pr) results in decreasing the velocity. For the time-step t = 40 temperature increases with Pr till y=4, after that it decreases far away from the wall.

Figure 13 evince the effect of heat source parameter S on temperature profiles. From the figure it is clear that when S increases then the temperature rises with different time steps.

The effects of Schmidt number (Sc) on the velocity and concentration profiles are described with different time-steps in Figure 6 and Figure 14. For the increasing value of Schmidt number the velocity is rising whereas mass concentration is falling.

Figure 7 and Figure 16 represent the effect of Chemical reaction parameter (R) on the velocity and mass concentration profiles. When R increases then the velocity and mass concentration are decreased.

The effect of Soret number (S_0) on the velocity, temperature and concentration profiles are shown in Figure 8, Figure 12 and Figure 15.From the Figure 8 it is shown that for the increasing value of S_0 the velocity is increasing for the time step t=1. And for the time steps t=5, t=40 the velocity decreases near the wall and again increases far away from the wall. Figure 12 shows that for t=1, 5 there is no effect of S_0 on temperature profiles, but for t=40 the temperature increases for an increasing value of Soret number. For the increasing value of S_0 mass concentration is increasing for t=1 and decreasing for t=5, 40 respectively.

The effects of magnetic field parameter M and Prandtl number Pr on streamlines and isotherm lines are described for the case of stream and water respectively. Streamlines can be obtained with the help of numerical integration of the following integral equation from 0 to Y_∞.

$$\psi = \int_0^{Y_\infty} U dY$$

The streamlines and isotherm lines for the values of magnetic field parameter M=2.0 and 4.0 are represented in the figure 17 and figure 19 while permeability parameter K, heat source parameter S, Prandtl number Pr takes the values 3.0, 0.5 and 0.71 respectively. Figure 17 (a) and 17 (b) show that the value of stream function within the computational domain decreases from 0.2635 to 0.2093 as M increases from 2.0 to 4.0. From this we may conclude that magnetic field opposes the flow of the fluid. Effects of the magnetic field on the development of isotherms explain in the figures 19 (a) and (b). The thermal boundary layer becomes thicker as M increases. It is clearly noticed that for all values of M, the temperature is increasing.

In the figures 18 (a) and (b) depicts the effect of Prandtl number on the development of streamlines and isotherm lines. From this figure it is observed that the stream function diminishes steadily from 0.2180 to 0.1751 for the increased value of Prandtl number. Also from the figure 20 the thermal boundary layer becomes thinner as increases of the Prandtl number.

The numerical value of skin-friction near the plate due to variation in Grashof number (Gr), modified Grashof number (Gm), magnetic field parameters (M), Schmidt number (Sc), permeability parameter (K), heat source parameter (S), Soret number (S_0), chemical reaction parameter (R) and Prandtl number (Pr) for externally cooled plate is given in Table 1. It is observed that an increase in Pr, R, Sc and M leads to decrease the skin-friction while an increase in Gr, Gm, K, S_0 and S results to increase the skin-friction.

Table 2 represents the numerical values of the Nusselt number for different values of Prandtl number (Pr), heat source parameter (S) and time-step (t). It is clear that for the increasing value of Pr the Nusselt number increases while an increase in t and S lead to decrease the values of Nusselt number.

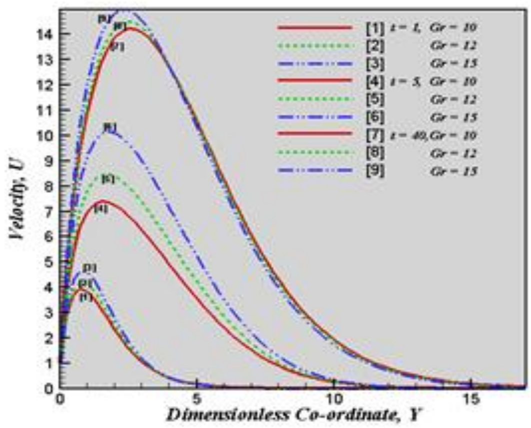

Figure 1. Velocity profiles for different values of Grashof number (*Gr*) against *Y*.

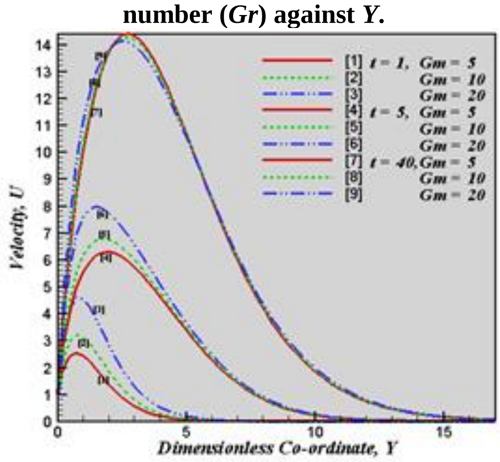

Figure 2. Velocity profiles for different values of modified Grashof number (Gm) against Y.

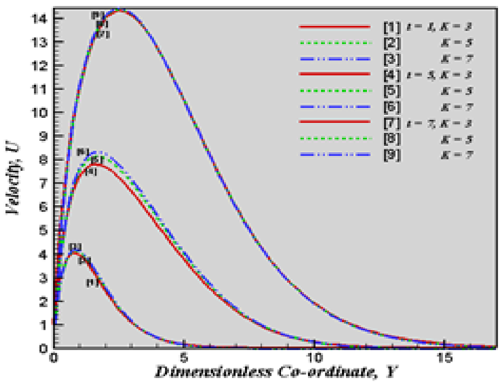

Figure 3. Velocity profiles for different values of permeability parameter (*K*) against *Y*.

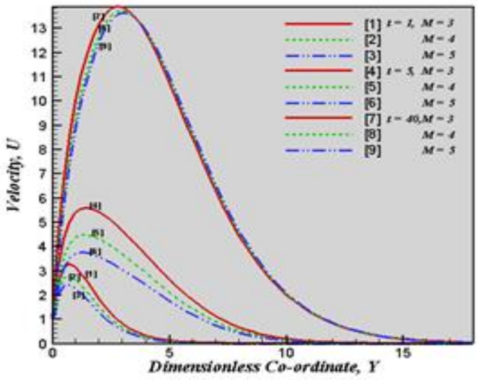

Figure 4. Velocity profiles for different values of magnetic field parameter (*M*) against *Y*.

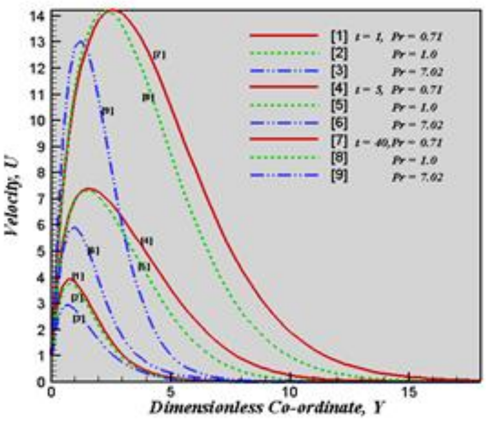

Figure 5. Velocity profiles for different values of Prandtl number (*Pr*) against *Y*.

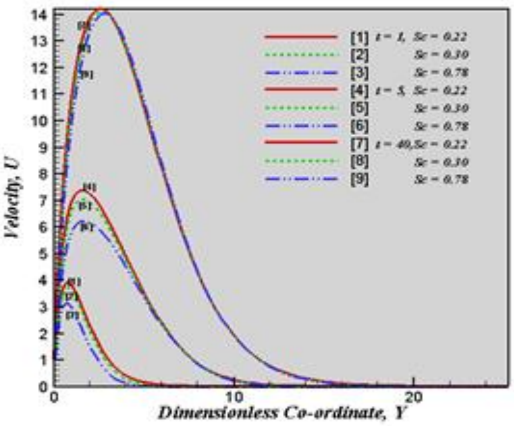

Figure 6. Velocity profiles for different values of Schmidth number (Sc) against Y.

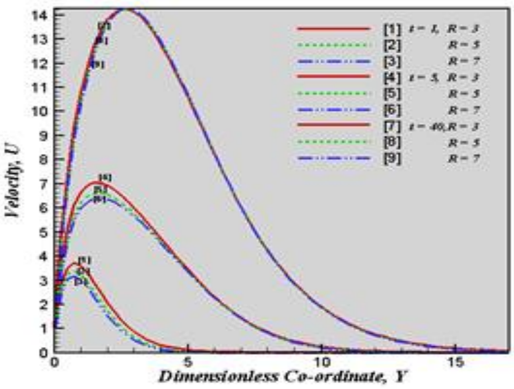

Figure 7. Velocity profiles for different values of chemical reaction parameter (*R*) against *Y*.

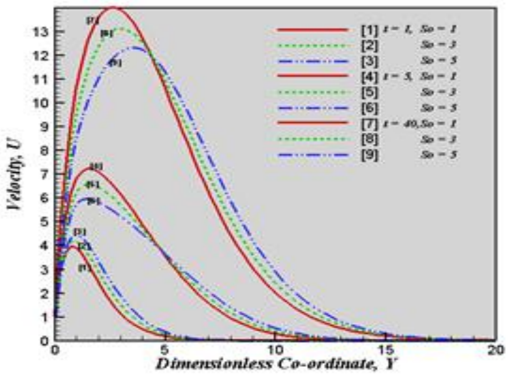

Figure 8. Velocity profiles for different values of soret number (S_0) against *Y*.

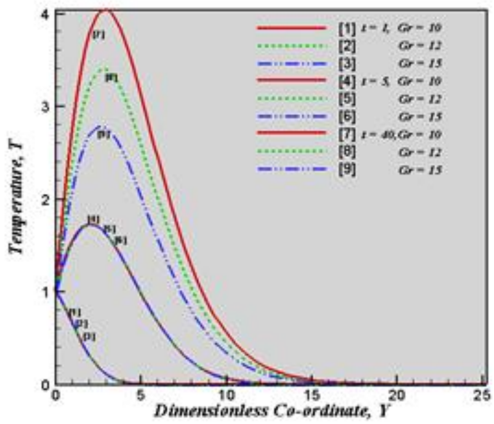

Figure 9. Temperature profiles for different values of Grashof number (*Gr*) against *Y*.

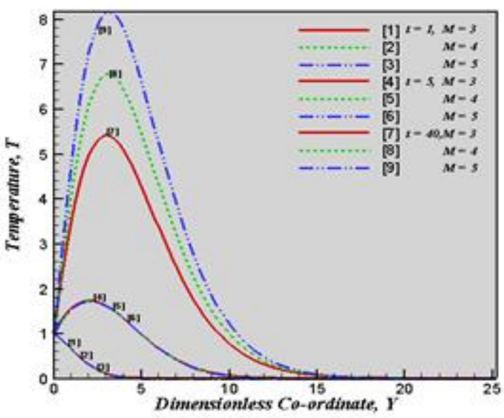

Figure 10. Temperature profiles for different values of magnetic field parameter (*M*) against *Y*.

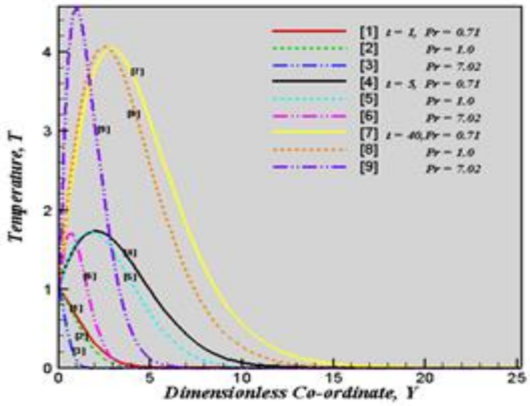

Figure 11. Temperature profiles for different values of Prandtl number (Pr) against Y.

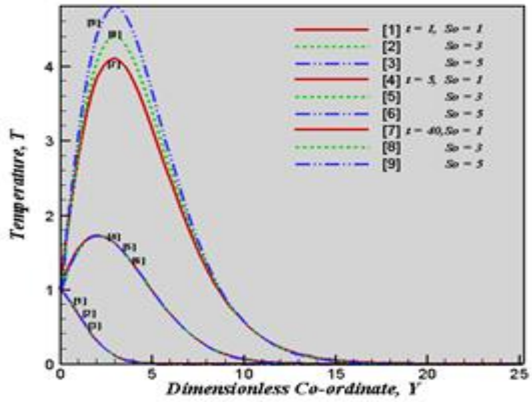

Figure 12. Temperature profiles for different values of soret number (S_0) against *Y*.

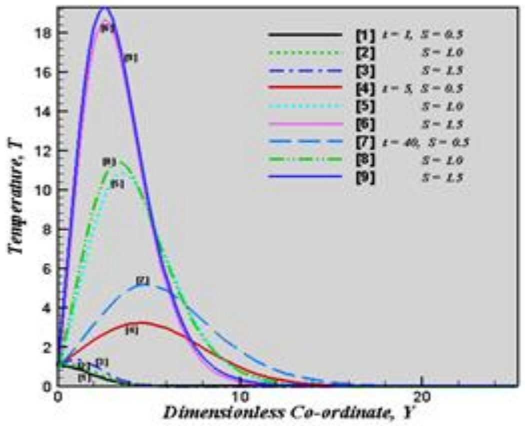

Figure 13. Temperature profiles for different values of heat source parameter (*S*) against *Y*.

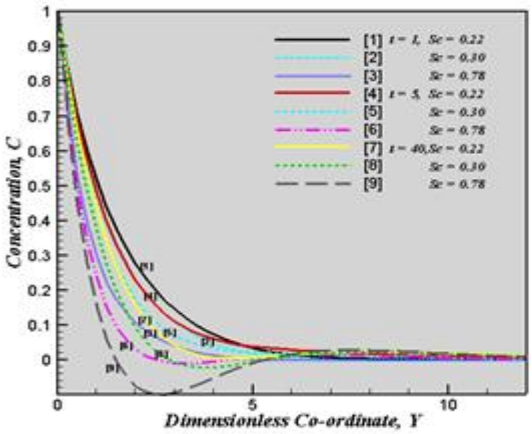

Figure 14. Concentration profiles for different values of Schmidth number (*Sc*) against *Y*.

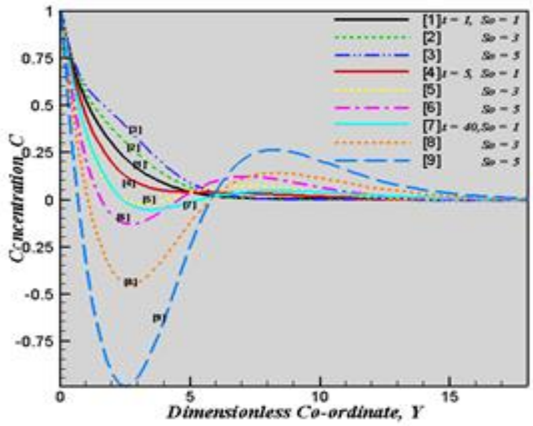

Figure 15. Concentration profiles for different values of Soret number (S_0) against *Y*.

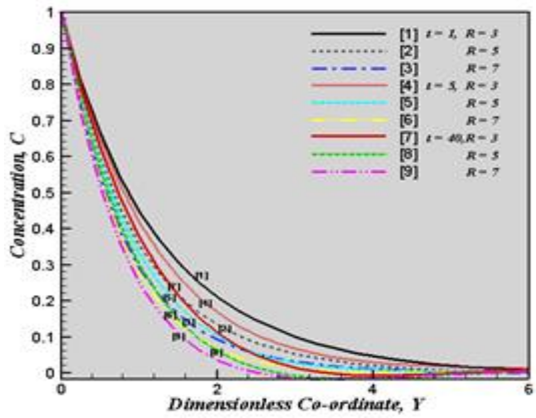

Figure 16. Concentration profiles for different values of chemical reaction parameter (*R*) against *Y*.

(a)

(b)

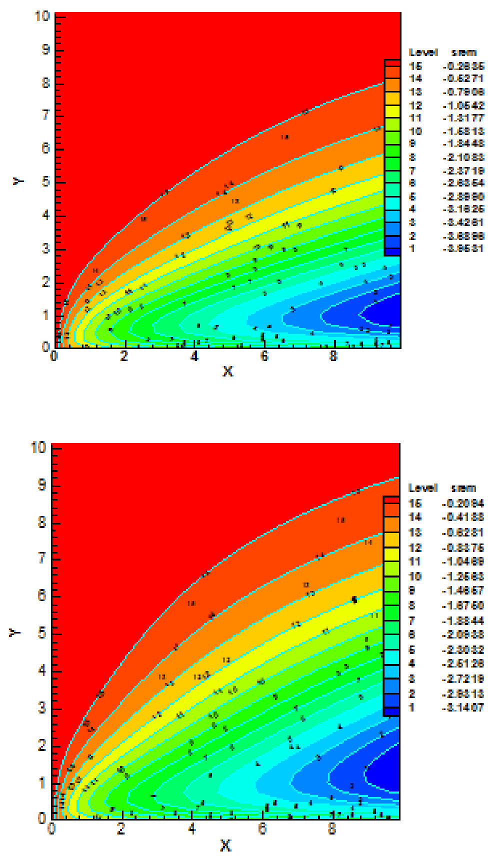

Figure 17. Streamlines for (a) *M*=2.0, (b) *M*=4.0 while *K*=3.0, *S*=0.5 and *Pr*=0.71.

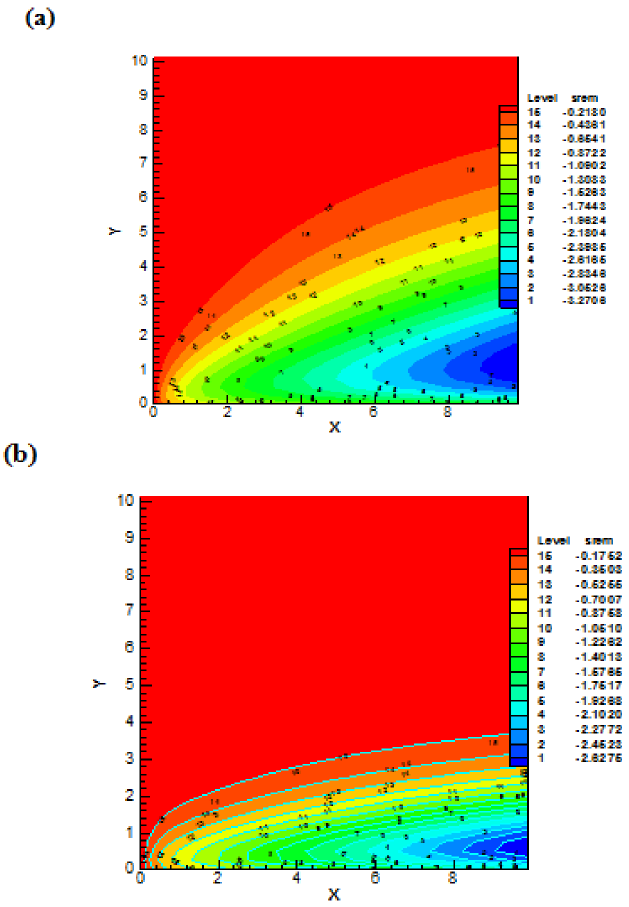

Figure 18. Streamlines for (a) Pr=1.0, (b) Pr=7.02 while K=3.0, S=0.5 and M=3.0.

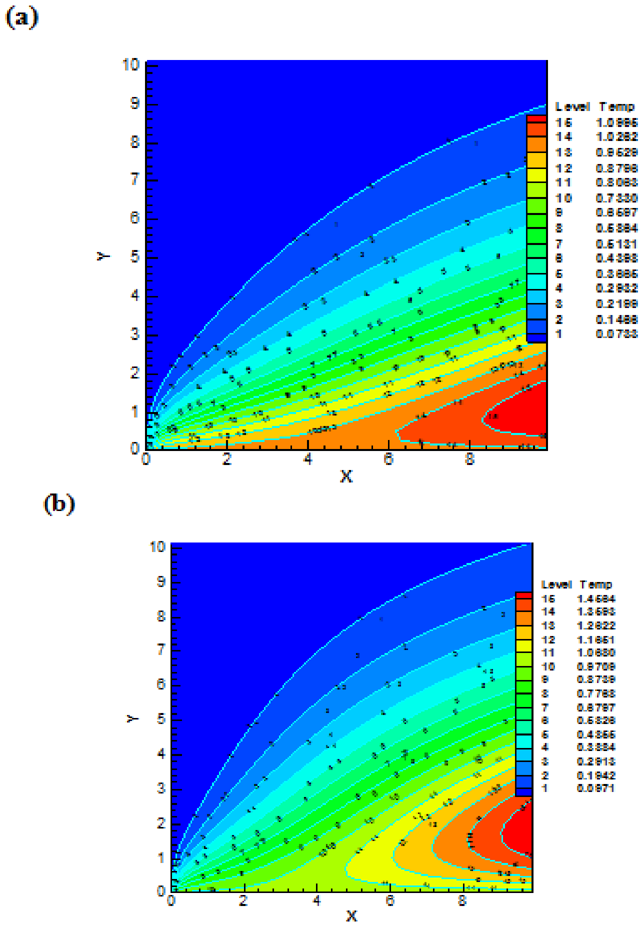

Figure 19. Isotherm lines for (a) M=2.0, (b) M=4.0 while K=3.0, S=0.5 and Pr=0.71.

Table 1. Numerical values of Skin-friction.

S. No.	*Gr*	*Gm*	*M*	*Sc*	*S*	*K*	S_0	*R*	*Pr*	Skin-friction
1.	10.0	5.0	3	0.22	0.5	3	1	3	0.71	0.8183456767
2.	10.0	5.0	3	0.22	0.5	3	1	3	7.02	0.6925601419
3.	10.0	5.0	3	0.22	0.5	3	1	5	0.71	0.8039190909
4.	10.0	5.0	3	0.22	0.5	3	3	3	0.71	0.8284034132
5.	10.0	5.0	3	0.22	0.5	5	1	3	071	0.8360476780
6.	10.0	5.0	3	0.22	1.5	3	1	3	0.71	2.9621371805
7.	10.0	5.0	3	0.78	0.5	3	1	3	0.71	0.7965244693
8.	10.0	5.0	5	0.22	0.5	3	1	3	0.71	0.6135142406
9.	10.0	10.0	3	0.22	0.5	3	1	3	0.71	1.0166683305
10.	15.0	5.0	3	0.22	0.5	3	1	3	0.71	0.8317059662

Table 2. Numerical values of Nusselt number.

S. No.	*Pr*	*S*	*t*	Nusselt Number
1.	0.71	0.5	40	-0.2718160222
2.	0.71	0.5	50	-0.2718724419
3.	0.71	0.5	80	-0.2719023976
4.	0.71	1.0	40	-1.0992584698
5.	0.71	1.5	40	-2.6651826578
6.	1.0	0.5	40	-0.2431539933
7.	7.02	0.5	40	-0.1150211192

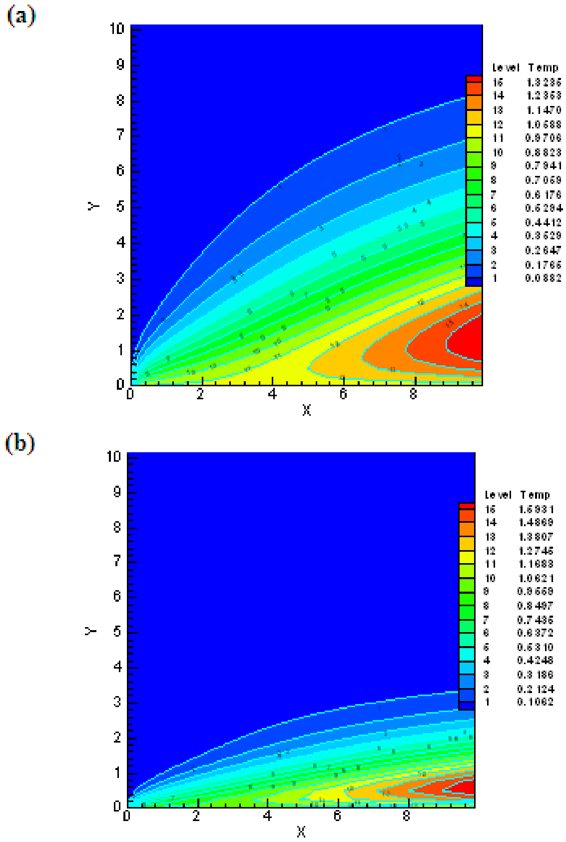

Figure 20. Isotherm lines for (a) *Pr*=1.0, (b) *Pr*=7.02 while *K*=3.0, *S*=0.5 and *M*=3.

Conclusion

The above study brings out the following inferences of physical interest on the velocity, temperature and concentration distribution as well as the streamlines, isotherm lines, skin friction and Nusselt number of the flow field.

- The velocity increases with increasing value of Grashof number (*Gr*), modified Grashof number (*Gm*) and Permeability parameter (*K*) whereas decreases with increasing value of magnetic field parameter (*M*), Prandtl number (*Pr*), Schmidth number (*Sc*), chemical reaction parameter (*R*) and soret number (S_0).
- The temperature increases with increasing value of magnetic field parameter (*M*), soret number (S_0) and heat source parameter (*S*) whereas decreases with increasing value of Grashof number (*Gr*) and Prandtl number (*Pr*).
- The mass concentration of fluid decreases with increasing value of Schmidth number (*Sc*), chemical reaction parameter (*R*) and soret number (S_0).
- For increasing values of *M* and *Pr*, the momentum and thermal boundary layer thickness enhanced.
- Skin friction increases with increasing value of Grashof number (*Gr*), modified Grashof number (*Gm*), Permeability parameter (*K*), soret number (S_0) and heat source parameter (*S*) whereas decreases with increasing value of magnetic field parameter (*M*), Prandtl number (*Pr*), Schmidth number (*Sc*), chemical reaction parameter (*R*).
- The values of Nusselt number increases with increasing value of Prandtl number (*Pr*) and decreases with an increasing value of *t* and *S*.

References

[1] Abd EL-Naby M. A., EI-BarbaryE. M. E. and N. Y. Abdelazem, “Finite difference solution of radiation effects on MHD unsteady free convection flow on vertical porous plate”, *Appl. Math. Comput. 151 (2)*, pp. 327-346,2004.

[2] S. F. Ahmmed, M. K. Das and L. E. Ali, “Analytical Study on Unsteady MHD Free Convection and Mass Transfer Flow past a Vertical Porous Plate.” *American Journal of Applied Mathematics.* Vol. 3, No. 2, 2015, pp. 64-74. doi : 10.11648/j.ajam.2015302.16

[3] S. S. Das, A. Satapathy, J. K. Das and J. P. Panda, “Mass transfer effects on MHD flow and heat transfer past a vertical porous plate through porous medium under oscillatory suction and heat source.” *International Journal of heat and Mass Transfer*, volume 52, Issues 25-26, December 2009, Pages 5962-5969.

[4] M Bhavana, D Chenna Kesavaish “The Soret Effect on free convective unsteady MHD Flow over a vertical plate with Heat Source.” *Int. Journal of Innovative Research in science and technology, Vol. 2,* May 2013.

[5] M. M. Alam, M. R. Islam and F. Rahman, “Micro-polar fluid behavior on MHD heat transfer flow through a porous medium with induced magnetic field by finite difference method.” *Int. J. of Science and Technology*, v.4, p.13, 2008.

[6] H. S. Takhar, P. Ganesan, K. Ekambavahar, V. M. Soundalgekar, “Transient free convection past a semi-infinite vertical plate with variable surface temperature.” *International Journal of Numerical Methods in Heat Fluid Flow*, v.7, p.280-296, 1997.

[7] U. S. Rajput and P. K. Sahu, “Effects of chemical reactions on free convection MHD flow past an exponentially accelerated infinite vertical plate through a porous medium with variable temperature and mass diffusion.” *Elixir Appl. Math.* 43 (2012) 6520-6527.

[8] J. Girish Kumar, P. M. Kishore, S. Ramakrishna, “Mass transfer effects on mhd flows exponentially accelerated isothermal vertical plate in the presence of chemical reaction through porous medium.” *Advances in Applied Science Research*, 2012, 3 (4):2134-2140.

[9] M. S. Hossain, S. K. Paul, S. F. Ahmmed and T. Sultana, “Study on MHD Free Convection Heat and Mass Transfer Flow past a Vertical Plate in the Presence of Hall Current

[10] N. Vedavathi, K. Ramakrishna, K. Jayarami Reddy, “Radiation and mass transfer effects on unsteady MHD convective flow past an infinite vertical plate with Dufour and Soret effects.” *Ain Shams Engineering Journal* (2015) 6, 363–371.

[11] B Gebhart, and L. Pera, “The nature of vertical natural convection flows resulting from the combined buoyancy effects of thermal and mass diffusion”, *Int. J. Heat Mass Transfer*, vol. 14, pp. 2025-2050, 1971.

[12] S. F, Ahmmed, S. Mondal and A. Ray, “MHD free convection and mass transfer flow past a vertical flat plate”, *Int. J. of Modern Engineering Research*, vol. 3, Issue. 1, pp. 75-82, 2013.